

Lepton polarization asymmetry and forward backward asymmetry in exclusive $B \rightarrow K_1 \tau^+ \tau^-$ decay in universal extra dimension scenario

Asif Saddique¹, M. Jamil Aslam^{2,3}, and Cai-Dian Lü²

¹*Department of Physics, Quaid-i-Azam University, Islamabad
and National Centre for Physics, Islamabad, Pakistan.*

²*Institute of High Energy Physic, P. O. Box 918(4), Beijing, 100049, P. R. China.*

³*COMSATS Institute of Information Technology Islamabad, Pakistan*

Decay rate, forward-backward asymmetry and polarization asymmetries of final state leptons in $B \rightarrow K_1 \tau^+ \tau^-$, where K_1 is the axial vector meson, are calculated in Standard Model and in the universal extra dimension (UED) model. The sensitivity of the observables on the compactification radius R , the only unknown parameter in UED model, is studied. Finally, the helicity fractions of the final state K_1 are calculated and their dependence on the compactification radius is discussed. This analysis of helicity fraction is briefly extended to $B \rightarrow K^* \ell^+ \ell^-$ ($\ell = e, \mu$) and compared with the other approaches exist in the literature.

I. INTRODUCTION

It is generally believed that Standard Model (SM) of particle physics is one of the most successful theory of the second half of previous century in explaining the observed data so far, but no one can say that it is the end of physics. Intensive search for physics beyond SM is now being performed in various areas of particle physics which is expected to get the direct evidence at high energy colliders such as the Large Hadron Collider (LHC). During the last years there has been an increased interest in models with extra dimensions, since they solve the hierarchy problem and can provide the unified framework of gravity and other interactions together with a connection with the string theory [1]. Among them a special role play the ones with universal extra dimensions (UED) as in these models all SM fields are allowed to propagate in all available dimensions. The economy of UED models is that there is only one new free parameter in addition to SM, the radius R of the compactified extra dimension. Now above the compactification scale $1/R$ a given UED model become a higher dimensional field theory whose equivalent description in four dimensions consists of SM fields, the towers of their Kaluza-Klein (KK) partners and additional towers of KK modes having no partner in SM. Appelquist, Cheng and Dobrescu (ACD) model [2], with one extra universal dimension is

the simplest model of this type. In this model the only additional free parameter relative to SM is the compactification scale $1/R$. Thus, all the masses of the KK particles and their interactions with SM particles and also among themselves are described in terms of $1/R$ and the parameters of SM [3].

The most profound property of ACD model is the conservation of KK parity which implies the absences of tree level contribution of KK states to the low energy processes taking place at scale $\mu \ll 1/R$. This brings interest towards the flavor-changing-neutral-current (FCNC) transitions $b \rightarrow s$, as these are not allowed at tree level but are induced by the Glashow-Iliopoulos-Miani (GIM) amplitudes [4] at the loop level in the SM and hence the one loop contribution due to KK modes to them could in principle be important. These processes are used to constrain the mass and couplings of KK states, i.e. the compactification parameter $1/R$ [5].

Buras and collaborators have computed the effective Hamiltonian of several FCNC processes in ACD model, particularly in b sector, namely $B_{s,d}$ mixing and $b \rightarrow s$ transition such as $b \rightarrow s\gamma$ and $b \rightarrow s\ell^+\ell^-$ [3]. The implications of physics with UED are being examined with the data from accelerator experiments, for example, from Tevatron experiments the bound on the inverse of compactification radius is found to be about $1/R \geq 300$ GeV [6]. Exclusive $B \rightarrow K(K^*)\ell^+\ell^-$, $B \rightarrow K(K^*)\nu\bar{\nu}$ and $B \rightarrow K^*\gamma$ decays are analyzed in ACD model and it was shown that the uncertainties connected with hadronic matrix elements does not mask the sensitivity to the compactification parameter, and the current data on the decay rates of $B \rightarrow K^*\gamma$ and $B \rightarrow K^*\ell^+\ell^-$ ($\ell = e, \mu$) can provide a similar bound to the inverse compactification radius: $1/R \geq 300 - 400$ GeV [7]. In addition to these the decay modes $B \rightarrow K_1\ell^+\ell^-$ ($\ell = e, \mu$), $B \rightarrow \phi\ell^+\ell^-$, $B \rightarrow \gamma\ell^+\ell^-$ and $\Lambda_b \rightarrow \Lambda\ell^+\ell^-$ have also been considered, with the possibility of observing such processes at hadron colliders [8, 9, 10].

Colangelo *et al.* have also considered another set of observables in FCNC transitions, namely those of the inclusive $B \rightarrow X_s + \text{leptons}$ and exclusive $B \rightarrow K(K^*) + \text{leptons}$ decay modes, where the leptons are $\tau^+\tau^-$ [11]. There is no experimental data on these days as yet, however as first noticed in [12], these processes are of great interest due to the possibility of measuring lepton polarization asymmetries which are sensitive to the structure of the interactions, so that they can be used to test the SM and its extensions. They analyzed the τ^- polarization asymmetries in single universal extra dimension model both for inclusive and exclusive semileptonic B meson decays. Besides this, they investigated another observable, the fraction of longitudinal K^* polarization in $B \rightarrow K^*\ell^+\ell^-$, for which a new measurement in two bins of momentum transfer to the lepton pair is available in case of $\ell = e, \mu$. They studied the dependence of this quantity on the compactification parameter,

for $B \rightarrow K^* \tau^+ \tau^-$ and in the case of light leptons, together with the fraction of K^* polarization in the same modes, and discussed the possibility to constrain the universal extra dimension scenario.

In this work, we will study the spin effects on $B \rightarrow K_1 \tau^+ \tau^-$ in ACD model using the framework of $B \rightarrow K^* \tau^+ \tau^-$ described by Colangelo *et al.* [11]. We investigate the branching ratio, forward backward and polarization asymmetries for the final state τ^- . Although the sensitivity of branching ratio and forward backward asymmetry on the extra dimension is mild but still we believe that together with the τ^- lepton polarization asymmetries, these can be used to provide additional constraints on the comactification parameter. In extension to this, we have also discussed, the fraction of longitudinal K^* polarization in $B \rightarrow K^* \ell^+ \ell^-$, for which new measurements in two bins of momentum transfer to the lepton pair is available in case of $\ell = e, \mu$ and compared them with the other approaches existed already in the literature [11]. Finally, we have used the same method to calculate the helicity fractions of K_1 in $B \rightarrow K_1 \ell^+ \ell^-$ both in SM and in ACD model. We hope that these fractions put another useful constraints on the universal extra dimension scenario.

The paper is organized as follows. In Section 2 we present the effective Hamiltonian for $B \rightarrow K_1 \ell^+ \ell^-$ in ACD model. In section 3, we will calculate the decay rate and forward backward asymmetry for $B \rightarrow K_1 \tau^+ \tau^-$. Section 4 and 5 deals with the study of polarization asymmetries of final state τ^- and the helicity fractions of final state K_1 meson, respectively. We will summarize our results at the last section.

II. EFFECTIVE HAMILTONIAN

At quark level the decay $B \rightarrow K_1 \ell^+ \ell^-$ is same like $B \rightarrow K^* \ell^+ \ell^-$ as discussed by Ali *et al.*[13], i.e. $b \rightarrow s \ell^+ \ell^-$ and it can be described by effective Hamiltonian obtained by integrating out the top quark and W^\pm bosons

$$H_{eff} = -4 \frac{G_F}{\sqrt{2}} V_{tb} V_{ts}^* \sum_{i=1}^{10} C_i(\mu) O_i(\mu) \quad (1)$$

where O_i 's are four local quark operators and C_i are Wilson coefficients calculated in Naive dimensional regularization (NDR) scheme [14].

One can write the above Hamiltonian in the following free quark decay amplitude

$$\mathcal{M}(b \rightarrow s \ell^+ \ell^-) = \frac{G_F \alpha}{\sqrt{2} \pi} V_{tb} V_{ts}^* \left\{ \begin{array}{l} C_9^{eff} [\bar{s} \gamma_\mu L b] [\bar{\ell} \gamma^\mu \ell] \\ + C_{10} [\bar{s} \gamma_\mu L b] [\bar{\ell} \gamma^\mu \gamma^5 \ell] \\ - 2 \hat{m}_b C_7^{eff} \left[\bar{s} i \sigma_{\mu\nu} \frac{\hat{q}^\nu}{\hat{s}} R b \right] [\bar{\ell} \gamma^\mu \ell] \end{array} \right\}, \quad (2)$$

with $L/R \equiv \frac{(1 \mp \gamma_5)}{2}$, $s = q^2$ which is just the momentum transfer from heavy to light meson. The amplitude given in Eq. (2) contains long distance effects encoded in the form factors and short distance effects that are hidden in Wilson coefficients. These Wilson coefficients have been computed at next-to-next leading order (NNLO) in the SM [15]. Specifically for exclusive decays, the effective coefficient C_9^{eff} can be written as

$$C_9^{eff} = C_9 + Y(\hat{s}) \quad (3)$$

where the hat denote the normalization in term of B meson mass. For the explicit expressions of $Y(\hat{s})$ is [14]

$$Y_{\text{pert}}(\hat{s}) = \frac{g(\hat{m}_c, \hat{s})(3C_1 + C_2 + 3C_3 + C_4 + 3C_5 + C_6) - \frac{1}{2}g(1, \hat{s})(4C_3 + 4C_4 + 3C_5 + C_6) - \frac{1}{2}g(0, \hat{s})(C_3 + 3C_4) + \frac{2}{9}(3C_3 + C_4 + 3C_5 + C_6)}{\quad} \quad (4)$$

Here the hat denote the normalization in term of B meson mass. For the explicit expressions of g 's and numerical values of the Wilson coefficients appearing in Eq. (4) we refer to [14].

Now the new physics effects manifest themselves in rare B decays in two different ways, either through new contribution to the Wilson coefficients or through the new operators in the effective Hamiltonian, which are absent in the SM. In ACD model the new physics comes through the Wilson coefficients. Buras et al. have computed the above coefficients at NLO in ACD model including the effects of KK modes [3]; we use these results to study $B \rightarrow K_1 \tau^+ \tau^-$ decay like the one done in the literature for $B \rightarrow K^*(K_1) \mu^+ \mu^-$ [7, 8]. As it has already been mentioned that ACD model is the minimal extension of SM with only one extra dimension and it has no extra operator other than the SM, therefore, the whole contribution from all the KK states is in the Wilson coefficients, i.e. now they depend on the additional ACD parameter, the inverse of compactification radius R . At large value of $1/R$ the SM phenomenology should be recovered, since the new states, being more and more massive, decoupled from the low-energy theory.

Now the modified Wilson coefficients in ACD model contain the contribution from new particles which are not present in the SM and comes as an intermediate state in penguin and box diagrams. Thus, these coefficients can be expressed in terms of the functions $F(x_t, 1/R)$, $x_t = \frac{m_t^2}{M_W^2}$, which generalize the corresponding SM function $F_0(x_t)$ according to:

$$F(x_t, 1/R) = F_0(x_t) + \sum_{n=1}^{\infty} F_n(x_t, x_n) \quad (5)$$

with $x_n = \frac{m_n^2}{M_W^2}$ and $m_n = \frac{n}{R}$ [7]. The relevant diagrams are Z^0 penguins, γ penguins, gluon penguins, γ magnetic penguins, Chromomagnetic penguins and the corresponding functions are

$C(x_t, 1/R)$, $D(x_t, 1/R)$, $E(x_t, 1/R)$, $D'(x_t, 1/R)$ and $E'(x_t, 1/R)$ respectively. These functions can be found in [3] and can be summarized as:

• C_7

In place of C_7 , one defines an effective coefficient $C_7^{(0)eff}$ which is renormalization scheme independent [14]:

$$C_7^{(0)eff}(\mu_b) = \eta^{\frac{16}{23}} C_7^{(0)}(\mu_W) + \frac{8}{3} (\eta^{\frac{14}{23}} - \eta^{\frac{16}{23}}) C_8^{(0)}(\mu_W) + C_2^{(0)}(\mu_W) \sum_{i=1}^8 h_i \eta^{\alpha_i} \quad (6)$$

where $\eta = \frac{\alpha_s(\mu_W)}{\alpha_s(\mu_b)}$, and

$$C_2^{(0)}(\mu_W) = 1, \quad C_7^{(0)}(\mu_W) = -\frac{1}{2} D'(x_t, \frac{1}{R}), \quad C_8^{(0)}(\mu_W) = -\frac{1}{2} E'(x_t, \frac{1}{R}); \quad (7)$$

the superscript (0) stays for leading logarithm approximation. Furthermore:

$$\begin{aligned} \alpha_1 &= \frac{14}{23} & \alpha_2 &= \frac{16}{23} & \alpha_3 &= \frac{6}{23} & \alpha_4 &= -\frac{12}{23} \\ \alpha_5 &= 0.4086 & \alpha_6 &= -0.4230 & \alpha_7 &= -0.8994 & \alpha_8 &= -0.1456 \\ h_1 &= 2.996 & h_2 &= -1.0880 & h_3 &= -\frac{3}{7} & h_4 &= -\frac{1}{14} \\ h_5 &= -0.649 & h_6 &= -0.0380 & h_7 &= -0.0185 & h_8 &= -0.0057. \end{aligned} \quad (8)$$

The functions D' and E' are given by eq. (8) with

$$D'_0(x_t) = -\frac{(8x_t^3 + 5x_t^2 - 7x_t)}{12(1-x_t)^3} + \frac{x_t^2(2-3x_t)}{2(1-x_t)^4} \ln x_t \quad (9)$$

$$E'_0(x_t) = -\frac{x_t(x_t^2 - 5x_t - 2)}{4(1-x_t)^3} + \frac{3x_t^2}{2(1-x_t)^4} \ln x_t \quad (10)$$

$$\begin{aligned} D'_n(x_t, x_n) &= \frac{x_t(-37 + 44x_t + 17x_t^2 + 6x_n^2(10 - 9x_t + 3x_t^2) - 3x_n(21 - 54x_t + 17x_t^2))}{36(x_t - 1)^3} \\ &+ \frac{x_n(2 - 7x_n + 3x_n^2)}{6} \ln \frac{x_n}{1 + x_n} \\ &- \frac{(-2 + x_n + 3x_t)(x_t + 3x_t^2 + x_n^2(3 + x_t) - x_n)(1 + (-10 + x_t)x_t)}{6(x_t - 1)^4} \ln \frac{x_n + x_t}{1 + x_n} \end{aligned} \quad (11)$$

$$\begin{aligned} E'_n(x_t, x_n) &= \frac{x_t(-17 - 8x_t + x_t^2 + 3x_n(21 - 6x_t + x_t^2) - 6x_n^2(10 - 9x_t + 3x_t^2))}{12(x_t - 1)^3} \\ &+ -\frac{1}{2} x_n(1 + x_n)(-1 + 3x_n) \ln \frac{x_n}{1 + x_n} \\ &+ \frac{(1 + x_n)(x_t + 3x_t^2 + x_n^2(3 + x_t) - x_n(1 + (-10 + x_t)x_t))}{2(x_t - 1)^4} \ln \frac{x_n + x_t}{1 + x_n} \end{aligned} \quad (12)$$

Following [3], one gets the expressions for the sum over n :

$$\begin{aligned}
\sum_{n=1}^{\infty} D'_n(x_t, x_n) = & -\frac{x_t(-37 + x_t(44 + 17x_t))}{72(x_t - 1)^3} \\
& + \frac{\pi M_w R}{2} \left[\int_0^1 dy \frac{2y^{\frac{1}{2}} + 7y^{\frac{3}{2}} + 3y^{\frac{5}{2}}}{6} \right] \coth(\pi M_w R \sqrt{y}) \\
& + \frac{(-2 + x_t)x_t(1 + 3x_t)}{6(x_t - 1)^4} J(R, -\frac{1}{2}) \\
& - \frac{1}{6(x_t - 1)^4} [x_t(1 + 3x_t) - (-2 + 3x_t)(1 + (-10 + x_t)x_t)] J(R, \frac{1}{2}) \\
& + \frac{1}{6(x_t - 1)^4} [(-2 + 3x_t)(3 + x_t) - (1 + (-10 + x_t)x_t)] J(R, \frac{3}{2}) \\
& - \frac{(3 + x_t)}{6(x_t - 1)^4} J(R, \frac{5}{2})], \tag{13}
\end{aligned}$$

$$\begin{aligned}
\sum_{n=1}^{\infty} E'_n(x_t, x_n) = & -\frac{x_t(-17 + (-8 + x_t)x_t)}{24(x_t - 1)^3} \\
& + \frac{\pi M_w R}{2} \left[\int_0^1 dy (y^{\frac{1}{2}} + 2y^{\frac{3}{2}} - 3y^{\frac{5}{2}}) \coth(\pi M_w R \sqrt{y}) \right] \\
& - \frac{x_t(1 + 3x_t)}{(x_t - 1)^4} J(R, -\frac{1}{2}) \\
& + \frac{1}{(x_t - 1)^4} [x_t(1 + 3x_t) - (1 + (-10 + x_t)x_t)] J(R, \frac{1}{2}) \\
& - \frac{1}{(x_t - 1)^4} [(3 + x_t) - (1 + (-10 + x_t)x_t)] J(R, \frac{3}{2}) \\
& + \frac{(3 + x_t)}{(x_t - 1)^4} J(R, \frac{5}{2})] \tag{14}
\end{aligned}$$

where

$$J(R, \alpha) = \int_0^1 dy y^\alpha [\coth(\pi M_w R \sqrt{y}) - x_t^{1+\alpha} \coth(\pi m_t R \sqrt{y})]. \tag{15}$$

• C_9

In the ACD model and in the NDR scheme one has

$$C_9(\mu) = P_0^{NDR} + \frac{Y(x_t, \frac{1}{R})}{\sin^2 \theta_W} - 4Z(x_t, \frac{1}{R}) + P_E E(x_t, \frac{1}{R}) \tag{16}$$

where $P_0^{NDR} = 2.60 \pm 0.25$ [14] and the last term is numerically negligible. Besides

$$\begin{aligned}
Y(x_t, \frac{1}{R}) &= Y_0(x_t) + \sum_{n=1}^{\infty} C_n(x_t, x_n) \\
Z(x_t, \frac{1}{R}) &= Z_0(x_t) + \sum_{n=1}^{\infty} C_n(x_t, x_n) \tag{17}
\end{aligned}$$

with

$$\begin{aligned}
Y_0(x_t) &= \frac{x_t}{8} \left[\frac{x_t - 4}{x_t - 1} + \frac{3x_t}{(x_t - 1)^2} \ln x_t \right] \\
Z_0(x_t) &= \frac{18x_t^4 - 163x_t^3 + 259x_t^2 - 108x_t}{144(x_t - 1)^3} \\
&\quad + \left[\frac{32x_t^4 - 38x_t^3 + 15x_t^2 - 18x_t}{72(x_t - 1)^4} - \frac{1}{9} \right] \ln x_t
\end{aligned} \tag{18}$$

$$C_n(x_t, x_n) = \frac{x_t}{8(x_t - 1)^2} [x_t^2 - 8x_t + 7 + (3 + 3x_t + 7x_n - x_t x_n) \ln \frac{x_t + x_n}{1 + x_n}] \tag{19}$$

and

$$\sum_{n=1}^{\infty} C_n(x_t, x_n) = \frac{x_t(7 - x_t)}{16(x_t - 1)} - \frac{\pi M_w R x_t}{16(x_t - 1)^2} \left[3(1 + x_t) J(R, -\frac{1}{2}) + (x_t - 7) J(R, \frac{1}{2}) \right] \tag{20}$$

• C_{10}

C_{10} is μ independent and is given by

$$C_{10} = -\frac{Y(x_t, \frac{1}{R})}{\sin^2 \theta_w}. \tag{21}$$

The normalization scale is fixed to $\mu = \mu_b \simeq 5 \text{ GeV}$.

III. DECAY RATE AND FORWARD BACKWARD ASYMMETRY

It is well known that Wilson coefficients give the short distance effects where as the long distance effects involve the matrix elements of the operators in Eq. (2) between the B and K_1 mesons in $B \rightarrow K_1 \tau^+ \tau^-$ process. Using standard parameterization in terms of the form factors we have [16]:

$$\begin{aligned}
\langle K_1(k, \varepsilon) | V_\mu | B(p) \rangle &= i\varepsilon_\mu^* (M_B + M_{K_1}) V_1(s) \\
&\quad - (p + k)_\mu (\varepsilon^* \cdot q) \frac{V_2(s)}{M_B + M_{K_1}} \\
&\quad - q_\mu (\varepsilon^* \cdot q) \frac{2M_{K_1}}{s} [V_3(s) - V_0(s)]
\end{aligned} \tag{22}$$

$$\langle K_1(k, \varepsilon) | A_\mu | B(p) \rangle = \frac{2i\varepsilon_{\mu\nu\alpha\beta}}{M_B + M_{K_1}} \varepsilon^{*\nu} p^\alpha k^\beta A(s) \tag{23}$$

where $V_\mu = \bar{s}\gamma_\mu b$ and $A_\mu = \bar{s}\gamma_\mu\gamma_5 b$ are the vector and axial vector currents respectively and ε_μ^* is the polarization vector for the final state axial vector meson.

The relationship between different form factors which also ensures that there is no kinematical singularity in the matrix element at $s = 0$ is

$$V_3(s) = \frac{M_B + M_{K_1}}{2M_{K_1}} V_1(s) - \frac{M_B - M_{K_1}}{2M_{K_1}} V_2(s) \tag{24}$$

$$V_3(0) = V_0(0). \tag{25}$$

In addition to the above form factors there are also some penguin form factors which are:

$$\begin{aligned} \langle K_1(k, \varepsilon) | \bar{s} i \sigma_{\mu\nu} q^\nu b | B(p) \rangle &= [(M_B^2 - M_{K_1}^2) \varepsilon_\mu^* - (\varepsilon^* \cdot q)(p + k)_\mu] F_2(s) \\ &+ (\varepsilon^* \cdot q) \left[q_\mu - \frac{s}{M_B^2 - M_{K_1}^2} (p + k)_\mu \right] F_3(s) \end{aligned} \quad (26)$$

$$\langle K_1(k, \varepsilon) | \bar{s} i \sigma_{\mu\nu} q^\nu \gamma_5 b | B(p) \rangle = -i \epsilon_{\mu\nu\alpha\beta} \varepsilon^{*\nu} p^\alpha k^\beta F_1(s) \quad (27)$$

with $F_1(0) = 2F_2(0)$.

Form factors are the non-perturbative quantities and are the scalar function of the square of momentum transfer. Different models are used to calculate these form factors. The form factors we use here in the analysis of the observables like decay rate, forward backward asymmetry and polarization asymmetries of final state τ in $B \rightarrow K_1 \tau^+ \tau^-$ have been calculated using Ward identities. The detailed calculation and their expressions are given in ref. [16] and can be summarized as:

$$\begin{aligned} A(s) &= \frac{A(0)}{(1 - s/M_B^2)(1 - s/M_B'^2)} \\ V_1(s) &= \frac{V_1(0)}{(1 - s/M_{B_A}^2)(1 - s/M_{B_A'}^2)} \left(1 - \frac{s}{M_B^2 - M_{K_1}^2} \right) \\ V_2(s) &= \frac{\tilde{V}_2(0)}{(1 - s/M_{B_A}^2)(1 - s/M_{B_A'}^2)} - \frac{2M_{K_1}}{M_B - M_{K_1}} \frac{V_0(0)}{(1 - s/M_B^2)(1 - s/M_B'^2)} \end{aligned} \quad (28)$$

with

$$\begin{aligned} A(0) &= -(0.52 \pm 0.05) \\ V_1(0) &= -(0.24 \pm 0.02) \\ \tilde{V}_2(0) &= -(0.39 \pm 0.03). \end{aligned} \quad (29)$$

The corresponding values for $B \rightarrow K^*$ form factors at $s = 0$ are given by [8]

$$\begin{aligned} V(0) &= (0.29 \pm 0.04) \\ A_1(0) &= (0.23 \pm 0.03) \\ \tilde{A}_2(0) &= (0.33 \pm 0.05). \end{aligned} \quad (30)$$

Following the notation from ref. [11], the differential decay rate in terms of the auxiliary functions can be written as

$$\frac{d\Gamma}{ds} = \frac{G_F^2 |V_{tb} V_{ts}^*|^2 \alpha^2 \lambda^{1/2}(M_B^2, M_{K_1}^2, s)}{2^{11} \pi^5} \frac{1}{3M_B^3 M_{K_1}^2 s} \sqrt{1 - \frac{4m_\tau^2}{s}} g(s) \quad (31)$$

TABLE I: Default value of input parameters used in the calculation

m_W	80.41 GeV
m_Z	91.1867 GeV
$\sin^2\theta_W$	0.2233
m_c	1.4 GeV
$m_{b,pole}$	4.8 ± 0.2 GeV
m_t	173.8 ± 5.0 GeV
$\alpha_s(m_Z)$	0.119 ± 0.0058
f_B	(200 ± 30) MeV
$ V_{ts}^* V_{tb} $	0.0385

where $\lambda(a, b, c) = a^2 + b^2 + c^2 - 2ab - 2bc - 2ca$ and the function $g(s)$ is:

$$\begin{aligned}
g(s) = & 24 |D_0|^2 m_\tau^2 M_{K_1}^2 \lambda + 8s M_{K_1}^2 \lambda \left[(2m_\tau^2 + s) |A|^2 - (4m_\tau^2 - s) |C|^2 \right] \\
& + \lambda \left[(2m_\tau^2 + s) |B_1 + (M_B^2 - M_{K_1}^2 - s) B_2|^2 - (4m_\tau^2 - s) \left| \begin{matrix} D_1 \\ + (M_B^2 - M_{K_1}^2 - s) D_2 \end{matrix} \right|^2 \right] \\
& + 4s M_{K_1}^2 \left[(2m_\tau^2 + s) (3 |B_1|^2 - \lambda |B_2|^2) - (4m_\tau^2 - s) (3 |D_1|^2 - \lambda |D_2|^2) \right]. \quad (32)
\end{aligned}$$

The auxiliary functions contain the short distance contribution (Wilson coefficients) as well as the long distance contribution (form factors):

$$\begin{aligned}
A &= 4(m_b + m_s) \frac{C_7^{eff}}{s} F_1(s) - \frac{A_0(s)}{M_B + M_{K_1}} C_9^{eff}(s) \\
B_1 &= (M_B + M_{K_1}) \left[C_9^{eff}(s) V_1(s) + \frac{4m_b}{s} C_7^{eff}(M_B - M_{K_1}) F_2(s) \right] \\
B_2 &= - \left[\frac{4m_b}{s} C_7^{eff} \left(F_2(s) + s \frac{F_3(s)}{M_B^2 - M_{K_1}^2} \right) + C_9^{eff}(s) \frac{V_2(s)}{M_B + M_{K_1}} \right] \\
C &= -C_{10} \frac{A(s)}{M_B + M_{K_1}} \\
D_0 &= C_{10} V_0(s) \\
D_1 &= C_{10} V_1(s) (M_B + M_{K_1}) \\
D_2 &= C_{10} \frac{V_2(s)}{M_B + M_{K_1}}. \quad (33)
\end{aligned}$$

Thus, integrating Eq. (31) on s and using the value of the form factors defined in Eq. (28), the numerical value of the branching ratio $B \rightarrow K_1 \tau^+ \tau^-$ is

$$B(B \rightarrow K_1 \tau^+ \tau^-) = (0.6 \pm 0.1) \times 10^{-7}.$$

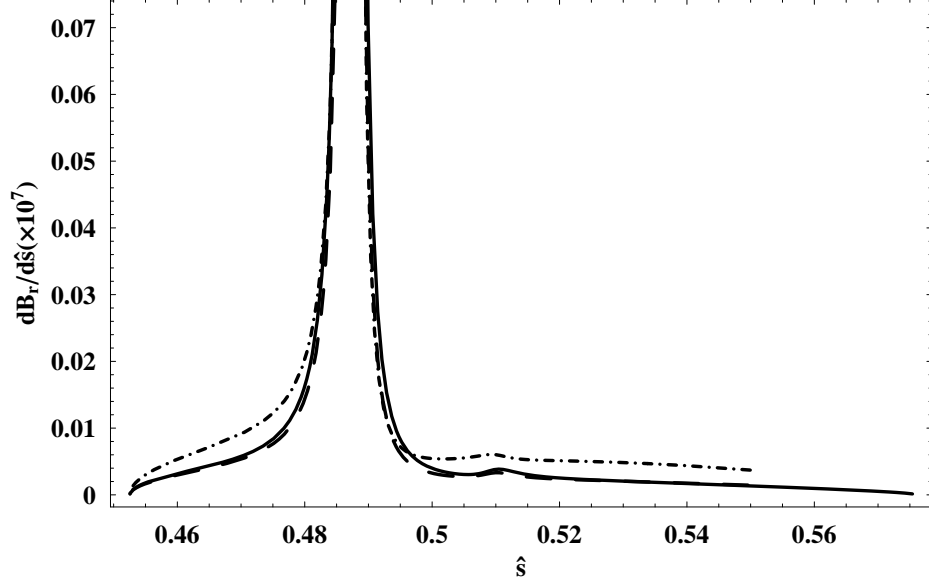


FIG. 1: The differential branching ratio as a function of \hat{s} is plotted using the form factors defined in Eq. (28). The solid line denotes the SM result, dashed-dotted line is for $1/R = 200$ GeV and dashed line is for $1/R = 500$ GeV. All the input parameters are taken at their central values.

The error in the value reflects the uncertainty from the form factors, and due to the variation of input parameters like CKM matrix elements, decay constant of B meson and masses as defined in Table I.

It is already mentioned that in ACD model there is no new operator beyond the SM and new physics will come only through the Wilson coefficients. To see this, the differential branching ratio against $\hat{s} (= s/M_B^2)$ is plotted in Fig. 1 using the central values of input parameters. One can see that the effect of KK contribution in the Wilson coefficient are modest for $1/R = 200$ GeV at low value of \hat{s} but such effects are obscured by the uncertainties involved in different parameters like, form factors, CKM matrix elements, etc at large value of \hat{s} .

Another observable is the forward backward asymmetry (\mathcal{A}_{FB}), which is also very useful tool for looking new physics. It has been shown by Ishtiaq *et al.* [8] that zero of the forward backward asymmetry is considerably shifted to the left in ACD model for $B \rightarrow K_1 \mu^+ \mu^-$. What we have shown in Fig. 2 is the differential forward backward asymmetry with \hat{s} for $B \rightarrow K_1 \tau^+ \tau^-$. Again the sensitivity of the zero on the extra dimension is very mild for $1/R = 200$ GeV.

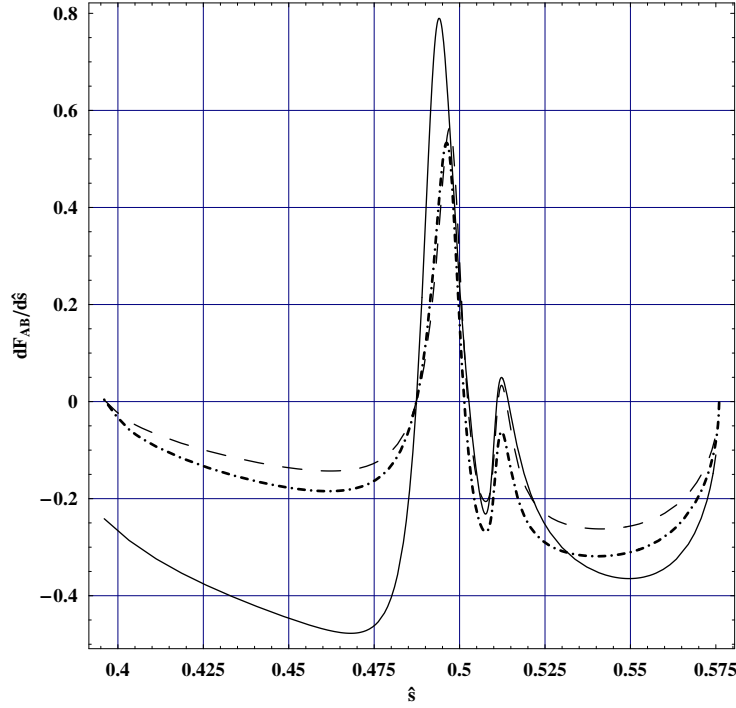


FIG. 2: The differential forward-backward (FB) asymmetry as a function of \hat{s} is plotted using the form factors defined in Eq. (28). The solid line denotes the SM result, dashed line is for $1/R = 200$ GeV and dashed-dotted line is for $1/R = 500$ GeV. All the input parameters are taken at their central values.

IV. POLARIZATION ASYMMETRIES OF FINAL STATE LEPTONS

In this section we will discuss the final state lepton polarization asymmetries by following the notation defined in ref. [11]. To compute these for B decays in τ leptons we consider the spin vector n of τ^- , with $n^2 = -1$ and $k_1 \cdot n = 0$, k_1 is the momentum of τ^- . Now in the rest frame of the τ^- lepton, one can define the three orthogonal unit vectors: e_L , e_N and e_T corresponding to the longitudinal n_L , normal n_N and transverse n_T polarization vectors:

$$\begin{aligned} n_L &= (0, e_L) = \left(0, \frac{\vec{k}_1}{|\vec{k}_1|}\right) \\ n_N &= (0, e_N) = \left(0, \frac{\vec{p} \times \vec{k}_1}{|\vec{p} \times \vec{k}_1|}\right) \\ n_T &= (0, e_T) = (0, e_N \times e_T) \end{aligned} \quad (34)$$

where, \vec{p} and \vec{k}_1 are the three momenta of K_1 and τ^- in the rest frame of the lepton pair. If we choose the z -axis as the momentum direction of τ^- in the rest frame of lepton pair, then $k_1 = (E_1, 0, 0, |\vec{k}_1|)$. Now boosting the spin vector n defined in Eq. (34) in the rest frame of lepton pair, the normal and transverse vectors n_N , n_T remains unchanged but the longitudinal

polarization vector changes. Their new form becomes

$$\begin{aligned} n_N &= (0, 1, 0, 0) \\ n_T &= (0, 0, -1, 0) \\ n_L &= \frac{1}{m_\tau} \left(|\vec{k}_1|, 0, 0, E_1 \right). \end{aligned} \quad (35)$$

The polarization asymmetry for negatively charged lepton τ^- for each value of the square of momentum transfer to the lepton pairs, s can be defined as:

$$\mathcal{A}_i(s) = \frac{\frac{d\Gamma}{ds}(n_i) - \frac{d\Gamma}{ds}(-n_i)}{\frac{d\Gamma}{ds}(n_i) + \frac{d\Gamma}{ds}(-n_i)} \quad (36)$$

with $i = L, T$ and N .

Thus, for $B \rightarrow K_1 \tau^+ \tau^-$ the expression of the longitudinal $\mathcal{A}_L(s)$ and transverse $\mathcal{A}_T(s)$ polarization asymmetries of τ^- becomes [11]:

$$\begin{aligned} \mathcal{A}_L(s) &= 2s \sqrt{1 - \frac{4m_\tau^2}{s}} \frac{1}{g(s)} \left\{ 8s M_{K_1}^2 \text{Re}[B_1 D_1^* + \lambda A C^*] \right. \\ &\quad \left. + \text{Re}[(M_B^2 - M_{K_1}^2 - s) B_1 + \lambda B_2] [(M_B^2 - M_{K_1}^2 - s) D_1^* + \lambda D_2^*] \right\} \end{aligned} \quad (37)$$

$$\mathcal{A}_T(s) = 3\pi m_\tau M_{K_1} \frac{\lambda \sqrt{s}}{g(s)} \left\{ -4 \text{Re}[A B_1^*] M_{K_1} s + \text{Re}[D_0 B_1^* (M_B^2 - M_{K_1}^2 - s) + \lambda D_0 B_2^*] \right\} \quad (38)$$

with $\lambda = \lambda(M_B^2, M_{K_1}^2, s)$. Now, while calculating these asymmetries we do not consider the contribution associated with the real $c\bar{c}$ resonances in C_9^{eff} , as these can be removed by using an appropriate kinematical cuts [11]. It is clear from Eq. (37) that the value of longitudinal polarization asymmetry vanishes when $s = 4m_\tau^2$. In Fig. 3 we have shown the effect of extra dimension on the value of the asymmetries. One can see that longitudinal polarization has the largest value at large momentum transfer (large value of \hat{s}) and is least sensitive to the compactification radius $1/R$. The effects of extra dimension are more evident for the transverse polarization whose value decreases with the decrease of $1/R$ down to $1/R = 200$ and the change is maximum for low value of \hat{s} .

V. HELICITY FRACTIONS OF K_1 IN $B \rightarrow K_1 \ell^+ \ell^-$

In this section, we study the helicity fractions of the K_1 produced in the final state, which is another interesting variable. For K^* meson, the longitudinal helicity fraction f_L in the modes

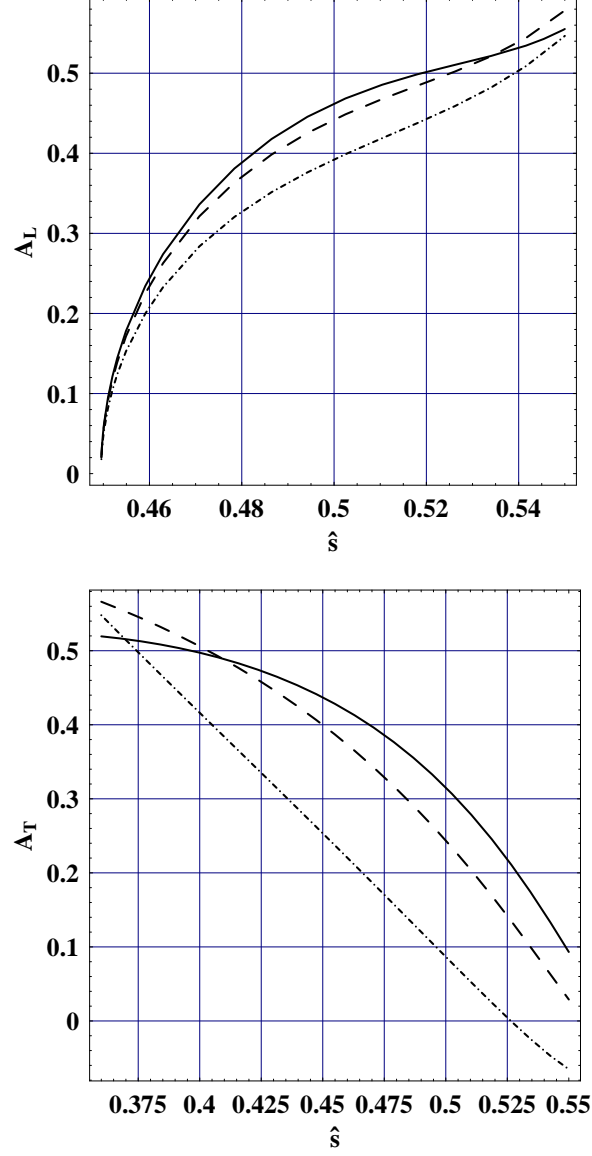


FIG. 3: Longitudinal (upper panel) and transverse (lower panel) τ^- polarization asymmetry in $B \rightarrow K_1 \tau^- \tau^+$ is plotted as a function of \hat{s} using form factor defined in Eq. (28). The solid line denotes the SM result, dashed line is for $1/R = 200$ GeV and long-dashed line is for $1/R = 500$ GeV. All the input parameters are taken at their central values.

$B \rightarrow K^* \ell^+ \ell^-$ ($\ell = e, \mu$), has been measured by Babar Collaboration in two bins of momentum transfer [17]. The results are:

$$\begin{aligned}
 f_L &= 0.77^{+0.63}_{-0.30} \pm 0.07 & 0.1 \leq s \leq 8.41 \text{ GeV}^2 \\
 f_L &= 0.51^{+0.22}_{-0.25} \pm 0.08 & s \geq 10.24 \text{ GeV}^2
 \end{aligned} \tag{39}$$

while the average value of f_L in the full s range is [11]

$$f_L = 0.63^{+0.18}_{-0.19} \pm 0.05 \quad s \geq 0.1 \text{ GeV}^2. \quad (40)$$

The expressions of $B \rightarrow K^* \ell^+ \ell^-$ differential decays widths with K^* longitudinal (L) or transversely (\pm) polarized are calculated by Colangelo et al. [11]. We will translate the same results for $B \rightarrow K_1 \ell^+ \ell^-$ as K^* and K_1 differ by γ_5 in their distribution amplitudes. The result reads as follows:

$$\begin{aligned} \frac{d\Gamma_L(s)}{ds} &= \frac{G_F^2 |V_{tb} V_{ts}^*|^2 \alpha^2 \lambda^{1/2} (M_B^2, M_{K_1}^2, s)}{2^{11} \pi^5 M_B^3} \sqrt{1 - \frac{4m_\ell^2}{s}} \frac{1}{3} A_L \\ \frac{d\Gamma_+(s)}{ds} &= \frac{G_F^2 |V_{tb} V_{ts}^*|^2 \alpha^2 \lambda^{1/2} (M_B^2, M_{K_1}^2, s)}{2^{11} \pi^5 M_B^3} \sqrt{1 - \frac{4m_\ell^2}{s}} \frac{4}{3} A_+ \\ \frac{d\Gamma_-(s)}{ds} &= \frac{G_F^2 |V_{tb} V_{ts}^*|^2 \alpha^2 \lambda^{1/2} (M_B^2, M_{K_1}^2, s)}{2^{11} \pi^5 M_B^3} \sqrt{1 - \frac{4m_\ell^2}{s}} \frac{4}{3} A_- \end{aligned} \quad (41)$$

with

$$\begin{aligned} A_L &= \frac{1}{s M_{K_1}^2} \{ 24 |D_0|^2 m_\ell^2 M_{K_1}^2 \lambda + (2m_\ell^2 + s) |(M_B^2 - M_{K_1}^2 - s) B_1 + \lambda B_2|^2 \\ &\quad + (s - 4m_\ell^2) |(M_B^2 - M_{K_1}^2 - s) D_1 + \lambda D_2|^2 \} \end{aligned} \quad (42)$$

and

$$\begin{aligned} A_- &= (s - 4m_\ell^2) \left| D_1 + \lambda^{1/2} C \right|^2 + (s + 2m_\ell^2) \left| B_1 + \lambda^{1/2} A \right|^2 \\ A_+ &= (s - 4m_\ell^2) \left| D_1 - \lambda^{1/2} C \right|^2 + (s + 2m_\ell^2) \left| B_1 - \lambda^{1/2} A \right|^2. \end{aligned} \quad (43)$$

The auxiliary functions and the corresponding form factors are defined in Eqs. (33) and (29). The various helicity amplitudes are defined as [11]:

$$\begin{aligned} f_L(s) &= \frac{d\Gamma_L(s)/ds}{d\Gamma(s)/ds} \\ f_\pm(s) &= \frac{d\Gamma_\pm(s)/ds}{d\Gamma(s)/ds} \\ f_T(s) &= f_+(s) + f_-(s). \end{aligned} \quad (44)$$

The helicity fractions for K^* has been considered in SM and some of its extensions [11, 18]. In Fig. 4 we have shown the results of the helicity fractions of K^* using the central value of the form factors and other parameters defined in ref. [8] in SM and for two values of the compactification radius $1/R$. The lepton in the final state is considered to be e or μ . The effect of extra dimensions are very mild for the low value of momentum transfer. One can see that the value of the longitudinal

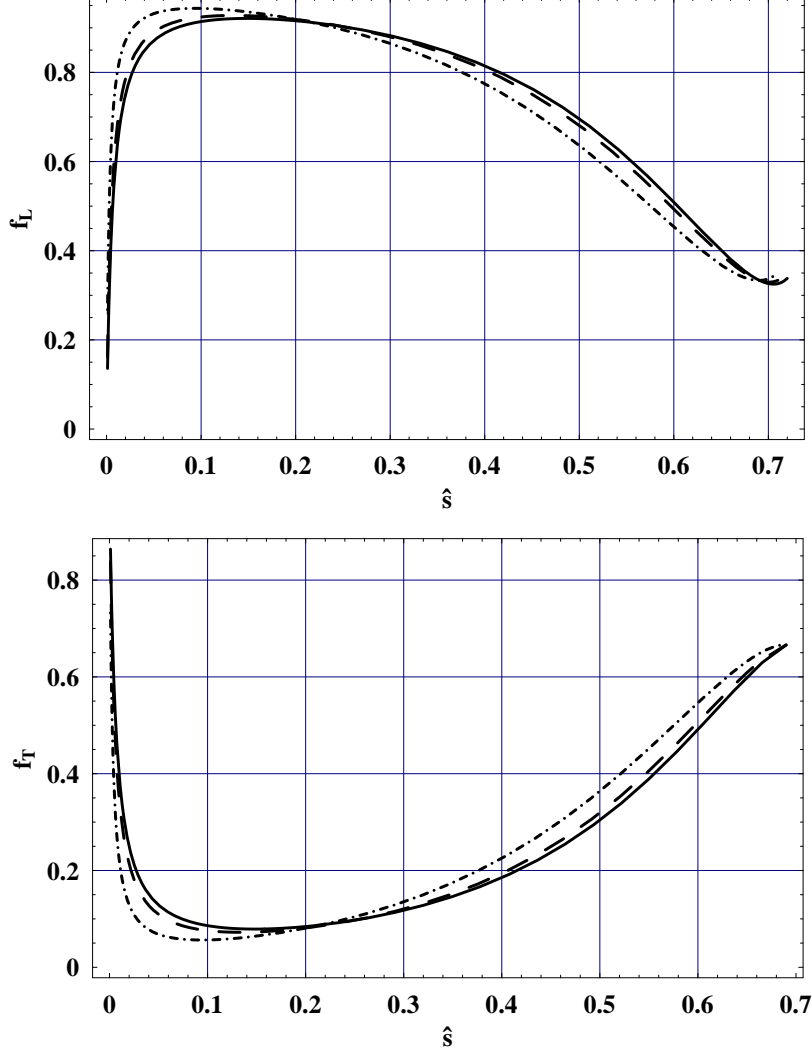


FIG. 4: : Longitudinal (upper panel) and transverse (lower panel) K^* helicity fractions in $B \rightarrow K^* \ell^- \ell^+$ ($\ell = e, \mu$) are obtained using form factor defined in Eq. (30). The solid line denotes the SM result, dashed line is for $1/R = 200$ GeV and long-dashed line is for $1/R = 500$ GeV. All the input parameters are taken at their central values.

helicity agrees with the experimental data within the experimental uncertainties both for the small and large value of momentum transfer. Thus, measurement of transverse helicity fraction will discriminate between the different models [11].

The results for the case of K_1 are shown in Fig. 5 and Fig. 6 in SM and in UED model for two values of $1/R$. Fig. 5 shows the helicity fractions of K_1 when we considered the e and μ as the final state lepton in $B \rightarrow K_1 \ell^+ \ell^-$ and take all the input parameters at their central values. One can see that the effect of extra dimension are very prominent at the small value of momentum transfer. These effects are constructive for the case of transverse helicity fraction and destructive

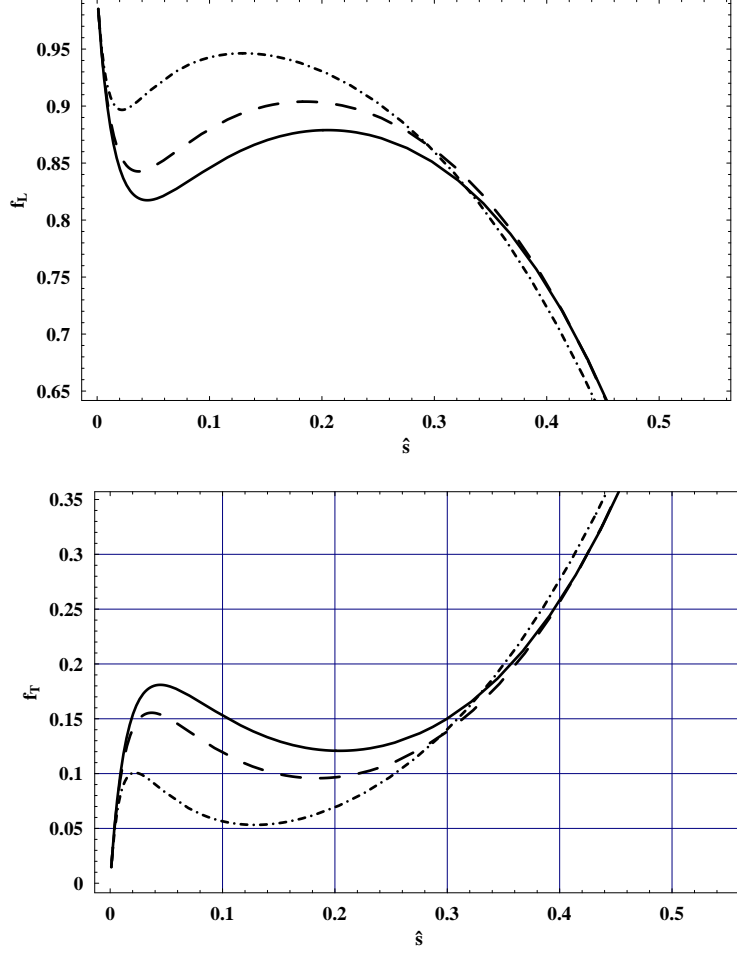


FIG. 5: Longitudinal (upper panel) and transverse (lower panel) K_1 helicity fractions in $B \rightarrow K_1 \ell^- \ell^+$ ($\ell = e, \mu$) are obtained using form factor defined in Eq. (28). The solid line denotes the SM result, dashed line is for $1/R = 200$ GeV and long-dashed line is for $1/R = 500$ GeV. All the input parameters are taken at their central values.

for the longitudinal one. Similarly, Fig. 6 depicts the results when we have considered the τ in the final state. Again, the effects of extra dimension are very modest at the small value of momentum transfers \hat{s} where f_L is maximum and f_T is minimum. From these two figures it is also clear that at each value of momentum transfer, $f_L(\hat{s}) + f_T(\hat{s}) = 1$. Thus we can say that the measurement of helicity fractions of K_1 will be possible in future B factories.

VI. CONCLUSION

In this paper, we have analyzed the spin effects in semileptonic decay $B \rightarrow K_1 \tau^+ \tau^-$ both in SM and in ACD model, which is minimal extension of SM with only one extra dimension. We

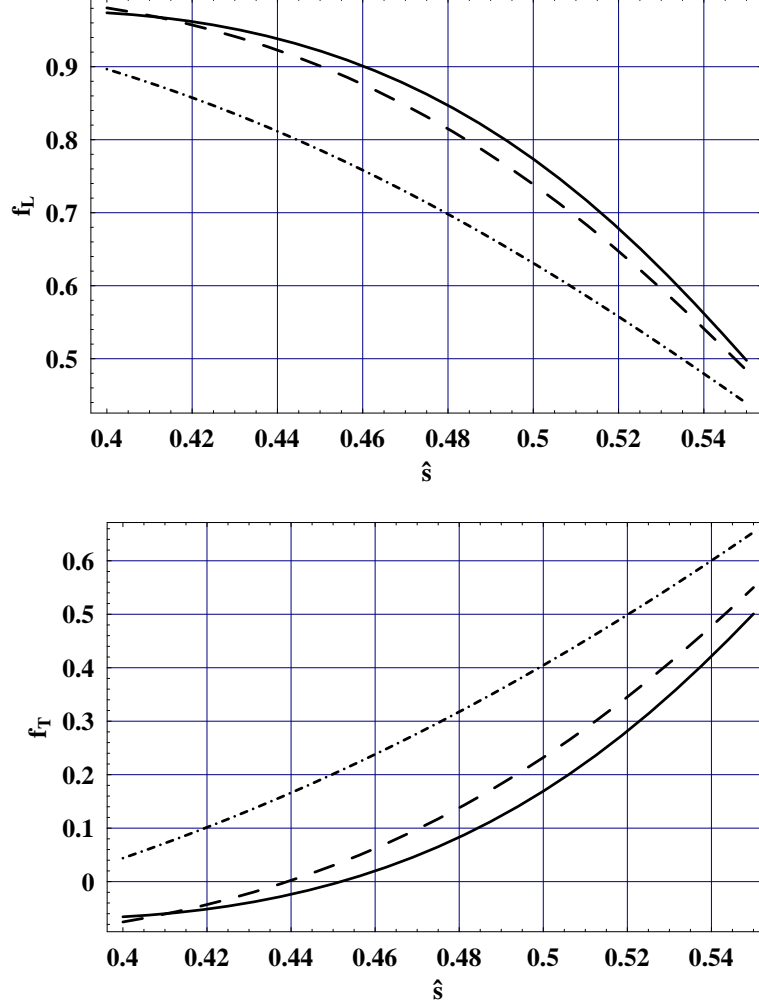


FIG. 6: Longitudinal (upper panel) and transverse (lower panel) K_1 helicity fractions in $B \rightarrow K_1 \tau^- \tau^+$ are obtained using form factor defined in Eq. (28). The solid line denotes the SM result, dashed line is for $1/R = 200$ GeV and long-dashed line is for $1/R = 500$ GeV. All the input parameters are taken at their central values.

studied the dependence of the physical observables like decay rate, forward backward asymmetry and polarization asymmetry on the inverse of compactification radius $1/R$. The effects of extra dimension to these observables are very mild, but still observable. Among the polarization asymmetries the most sensitive is the transverse one, where the effects of extra dimension for $1/R = 200$ GeV are very clear in the low momentum transfer range. K^* helicity fractions, for which some results for e and μ in the final state are already available have also been discussed and compared with the existing results in the literature. Finally, following the same analogy we considered the K_1 helicity fractions both in SM and in ACD model. The future experiments, where more data is expected, will put stringent constraints on the compactification radius and also give us some deep

understanding of B -physics and take us step forward towards the ultimate theory of fundamental interactions.

Acknowledgements

This work of Jamil and Lu is partly supported by National Science Foundation of China under the Grant Numbers 10735080 and 10625525. One of us (Asif) would like to thank Riazuddin, Fayyazuddin, Ishtiaq and Ali for useful discussions.

-
- [1] I. Antoniadis, Phys. Lett. **B246**, 377 (1990); K. R. Dienes, E. Dudas and T. Gherghetta, Phys. Lett. **B436**, 55 (1998); N. Arkani-Hamed and M. Schmaltz, Phys. Rev. **D61**, 033005 (2000); N. Arkani-Hamed, S. Dimopoulos and G. R. Dvali, Phys. Lett. **B429**, 263 (1998); L. Randall and R. Sundrum, Phys. Rev. Lett. **83**, 3370 (1999); L. Randall and R. Sundrum, Phys. Rev. Lett. **83**, 4690 (1999)
 - [2] T. Appelquist, H. C. Cheng and B. A. Dobrescu, Phys. Rev. **D64**, 035002 (2001).
 - [3] A. J. Buras, M. Spranger and A. Weiler, Nucl. Phys. **B660**, 225 (2003); A. J. Buras, A. Poschenrieder, M. Spranger and A. Weiler, Nucl. Phys. **B678**, 455 (2004).
 - [4] S. L. Glashow, J. Iliopoulos, and L. Maiani, Phys. Rev. **D2**, 1285 (1970).
 - [5] K. Agashe, N. G. Deshpande and G. H. Wu, Phys. Lett. **B514**, 309 (2001).
 - [6] T. Appelquist and H. U. Yee, Phys. Rev. **D67**, 055002 (2003).
 - [7] P. Colangelo, F. De Fazio, R. Ferrandes and T. N. Pham, Phys. Rev. **D73**, 115006 (2006).
 - [8] Ishtiaq Ahmed, M. Ali Paracha, M. Jamil Aslam, arXiv: hep-ph/0802.0740
 - [9] R. Mohanta and A. K. Giri, Phys.Rev.**D75**, 035008 (2007), arXiv: hep-ph/0611068.
 - [10] T. M. Aliev and M. Savci, arXiv:hep-ph/0606225; T. M. Aliev, M. Savci and B. B. Sirvanli, arXiv:hep-ph/0608143.
 - [11] P. Colangelo, F. De Fazio, R. Ferrandes, T. H. Pham, Phys.Rev.**D74**,115006 (2006), arXiv: hep-ph/0610044.
 - [12] J. L. Hewett, Phys. Rev. **D53**, 4964 (1996).
 - [13] A. Ali, P. Ball, L. T. Handoko and G. Hiller, Phys. Rev. **D61**, 074024 (2000) [arXiv:hep-ph/9910221].
 - [14] A. J. Buras *et al.*, Nucl. Phys. **B424**, 374 (1994).
 - [15] C. Bobeth, M. Misiak and J. Urban, Nucl. Phys. **B574**, 291 (2000); H. H. Asatrian, H. M. Asatrian, C. Greub and M. Walker, Phys. Lett. **B507**, 162 (2001); Phys. Rev. **D65**, 074004 (2002); Phys. Rev. **D66**, 034009 (2002); H. M. Asatrian, K. Bieri, C. Greub and A. Hovhannisyan, Phys. Rev. **D66**, 094013 (2002); A. Ghinculov, T. Hurth, G. Isidori and Y. P. Yao, Nucl. Phys. **B648**, 254 (2003); A. Ghinculov, T. Hurth, G. Isidori and Y. P. Yao, Nucl. Phys. **B685**, 351 (2004); C. Bobeth, P. Gambino, M. Gorbahn and U. Haisch, JHEP **0404**, 071 (2004).

- [16] M. Ali Paracha, Ishtiaq Ahmed and M. Jamil Aslam, Eur. Phys. J. **C52**, 967-973 (2007)
- [17] B. Aubert et al. [BABAR Collaboration], Phys. Rev. **D73**, 092001 (2006).
- [18] T. M. Aliev, A. Ozpineci and M. Savci, Phys. Lett. **B511**, 49 (2001).